

## Emittance Growth and Image Formation in a Nonuniform Space-Charge-Dominated Electron Beam

M. Reiser,<sup>(a,b)</sup> C. R. Chang,<sup>(a)</sup> D. Kehne,<sup>(a)</sup> K. Low,<sup>(b)</sup> and T. Shea<sup>(b)</sup>

*Laboratory for Plasma Research, University of Maryland, College Park, Maryland 20742*

H. Rudd

*Berkeley Research Associates, Springfield, Virginia 22150*

I. Haber

*Naval Research Laboratory, Washington, D.C. 20375*

(Received 23 June 1988)

An experiment was designed to check theoretical predictions of charge homogenization and emittance growth in nonuniform space-charge-dominated beams due to conversion of field energy into transverse kinetic energy. Five beamlets were masked out of a solid 5-keV electron beam and injected into a periodic solenoidal focusing channel. Phosphor screen images showed that the beamlets merged into an almost uniform density single beam. Images of the five-beamlet configuration were observed at a distance of 7–8 lens periods. Experimental results on merging distance and emittance growth were compared with theory and simulation and good agreement was found.

PACS numbers: 52.40.Mj, 29.15.-n, 52.25.Wz

Recent theoretical work and particle simulation studies on transport of intense beams in linear focusing channels have identified nonuniform charge distribution as a major cause of emittance growth.<sup>1–4</sup> This effect is of fundamental importance in advanced accelerator applications requiring intense high-brightness beams, such as free-electron lasers, H<sup>-</sup> linacs, heavy-ion fusion, relativistic klystrons for future e<sup>+</sup>e<sup>-</sup> linear colliders, etc. Recent studies at Berkeley on the merging of four ion beams indicate the significance of this effect in heavy-ion fusion and show good agreement between theoretical estimates and preliminary measurements of emittance growth.<sup>5</sup>

According to the theory, a nonuniform beam has higher field energy than the equivalent uniform beam, and the particle distribution will become uniform. The difference in field energy  $U$  is converted into transverse kinetic energy and hence emittance growth. Simulation<sup>2</sup> and theory<sup>3</sup> show that this effect occurs in a distance of  $\lambda_p/4$ , where  $\lambda_p = 2\pi v/\omega_p$  is the beam plasma period and  $\omega_p = (q^2 n/\epsilon_0 \gamma m_0)^{1/2}$  is the plasma frequency, with  $\gamma = (1 - \beta^2)^{-1/2}$  the relativistic mass factor,  $v$  the particle velocity,  $c$  the speed of light,  $\beta = v/c$ ,  $m_0$  the rest mass, and  $q$  the charge of the particles.

Consider a continuous nonuniform beam with current  $I$ , particle kinetic energy  $(\gamma - 1)m_0 c^2$ , rms width  $\tilde{x} = \tilde{y}$ , and rms emittance  $\tilde{\epsilon}_x = \tilde{\epsilon}_y = \tilde{\epsilon}$  launched into a linear focusing channel with a conducting tube of radius  $b$ . Compare it with the equivalent uniform beam having the same parameters. In a periodic channel with period length  $S$ , the particle motion is pseudoharmonic and characterized by the phase advance per period  $\sigma$  of the oscillation wavelength  $\lambda$  defined as  $\sigma = 2\pi S/\lambda$  with self-

fields and  $\sigma_0 = 2\pi S/\lambda_0$  without self-fields.

It will be convenient to introduce<sup>6</sup> the effective radius  $R = 2\tilde{x}$ , and the effective emittance  $\epsilon = 4\tilde{\epsilon}$ , and to use the generalized perveance defined as  $K = (I/I_0)(2/\beta^3 \gamma^3)$ , where  $I_0 = 4\pi\epsilon_0 m_0 c^3/q \approx 1.7 \times 10^4$  A for electrons. From the smooth-approximation theory for periodic focusing of intense beams<sup>7</sup> one obtains the relationship

$$\frac{KR^2}{\epsilon^2} = \frac{\sigma_0^2}{\sigma^2} - 1. \quad (1)$$

According to the theory of emittance growth, the ratio of final emittance  $\epsilon_f$  to initial emittance  $\epsilon_i$  is given by

$$\frac{\epsilon_f}{\epsilon_i} = \left[ 1 + \frac{U}{2w_0} \left( \frac{\sigma_0^2}{\sigma^2} - 1 \right) \right]^{1/2}, \quad (2)$$

or, in view of (1) in the alternate form

$$\frac{\epsilon_f}{\epsilon_i} = \left( 1 + \frac{KR^2}{2\epsilon_i^2} \frac{U}{w_0} \right)^{1/2}, \quad (3)$$

where  $w_0 = \mu_0 I^2 / 16\pi\beta^2$  and  $U/w_0$  is a dimensionless quantity that depends only on the shape of the nonuniform distribution. Equation (1) was obtained by Struckmeier, Klabunde, and Reiser in Ref. 1. The differential equation for this emittance growth was first derived by Lapostolle<sup>6</sup> and independently by Wangler *et al.* (in Ref. 2).

The charge homogenization distance  $z_p = \lambda_p/4$  can be expressed as

$$z_p = \frac{\lambda_p}{4} = \frac{\pi v}{2\omega_p} = \frac{\pi R}{2(2K)^{1/2} \gamma}. \quad (4)$$

Our experiment was conducted in the beam transport system at the University of Maryland<sup>8</sup> in which a 5-keV electron beam from a 1-in.-diam thermionic cathode is transported through a periodic channel of 38 solenoid lenses, the first two being used to match the beam. The length of one lens period is 13.6 cm. Five small beamlets were masked out of the full 240-mA beam at the anode.

Figure 1 illustrates the experimental setup near the electron gun of the system. The measured current was 44 mA corresponding to  $K = 1.88 \times 10^{-3}$ . The emittance is measured at the end of the channel by a slit-pinhole system with a Faraday cup. A trolley can move a phosphor screen along the entire channel to within 3 cm of the aperture plate. The screen picture is recorded with a charge-coupled video camera.

The initial effective radius  $R_i$  and initial emittance  $\epsilon_i$  of the five-beamlet configuration shown in Fig. 1 are calculated to be

$$R_i = [a^2 - 1.6\delta^2]^{1/2} = 3.924a = 4.67 \text{ mm}, \quad (5)$$

$$\epsilon_i = R_i(2kT/eV_0)^{1/2} = 32.4 \text{ mm-mrad}, \quad (6)$$

where  $kT = 0.12 \text{ eV}$  is the cathode temperature and  $eV_0 = 5 \text{ keV}$  is the electron energy,  $a = 1.19 \text{ mm}$  is the beamlet radius, and  $\delta = 3a$  is the beamlet separation (see Fig. 1).

For the nonuniform field geometry factor  $U/w_0$ , one obtains the result

$$\frac{U}{w_0} = 0.16 \left\{ 5 - \ln \left[ \left( \frac{\delta}{a} \right)^5 \left( \frac{1-s^8}{4} \right)^4 \left( \frac{t^2 + 1.6s^2}{s^2} \right)^{12.5} \right] \right\} = 0.2656, \quad (7)$$

where  $s = \delta/b$ ,  $t = a/b$ , and  $b = 14 \text{ mm}$  is the pipe radius. The phase advance was set at  $\sigma_0 = 70^\circ$ . From the smooth-approximation theory<sup>7</sup> one then calculates an effective mean radius of  $R = 4.88 \text{ mm}$  and a phase advance with self-fields of  $\sigma = 0.15\sigma_0 \approx 10.6^\circ$  for the equivalent uniform beam. With these values, one finds from (2) for the emittance growth  $\epsilon_f/\epsilon_i = 2.6$  and from (4) for the merging distance  $z_p = 12.4 \text{ cm}$ .

Self-consistent particle-in-cell simulations have been performed with the two-dimensional SHIFT-XY code described elsewhere.<sup>9</sup> The magnetic field was represented by an analytical fit to the measured field profile on axis and by a fourth-order Taylor expansion for the off-axis components. Adequate accuracy was obtained with 32 time steps per lens period and  $\approx 32 \times 10^4$  particles on a  $256 \times 256$  mesh.

Figure 2 shows phosphor-screen pictures of the beam and the corresponding point plots from the simulation for the five beamlets at  $z = 3.4 \text{ cm}$ , the beam after charge homogenization at  $z = 17 \text{ cm}$ , and the image at  $z = 101 \text{ cm}$ . Note that the central beamlet in the experiment has lower density than the outer beamlets whereas the simulation assumed a constant-density beam. Figure 3 shows the magnetic field profile  $B(z)$  on the axis (top), and the simulation results for the beam radius and the emittance over a distance of about ten lens periods (bottom). The peak field in the periodic channel at  $\sigma_0 = 70^\circ$  was 83.2 G, and the Larmor rotation per lens was  $45^\circ$ . The radius

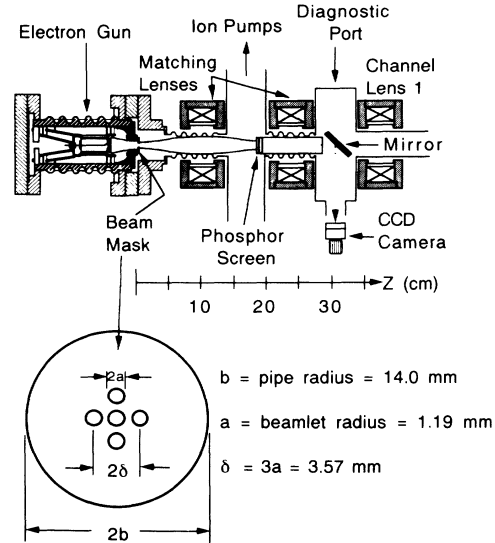


FIG. 1. Schematic of the multiple-beam experiment.

oscillations show that the beam was not perfectly matched. The emittance growth in the simulation is  $\epsilon_f/\epsilon_i = 2.6 \pm 0.1$  and occurs over a distance of about 15.5 cm. Experimental pictures and simulation plots show that the five beamlets merge into an almost uniform single beam at a distance of 14–17 cm. As can be seen from Fig. 2, the structure of the original beamlet configuration is still faintly visible at  $z = 17 \text{ cm}$ .

An unexpected effect was the appearance of images of the initial five-beamlet configuration at a distance between about 85 and 115 cm from the aperture plate, corresponding to approximately 6.5 to 8.5 lens periods. The best image was obtained at  $z = 101 \text{ cm}$ , or  $z \approx 7.5S$ , and is shown in fig. 2. The simulation runs also show some evidence of image formation but much fainter than the screen picture. We believe that the agreement can be improved by more detailed modeling of the experimental conditions. It is interesting to note that the small dip in the emittance curve of Fig. 3 near  $z = 100 \text{ cm}$  correlates with the image.

The image formation indicates that despite the charge homogenization and emittance growth, the beam retains some phase coherence and information about its origin. (The relationship between emittance, information, and entropy in charged particle beams was pointed out in a paper by Lawson, Lapostolle, and Gluckstern.<sup>10</sup> Furthermore, the image location provides information on the

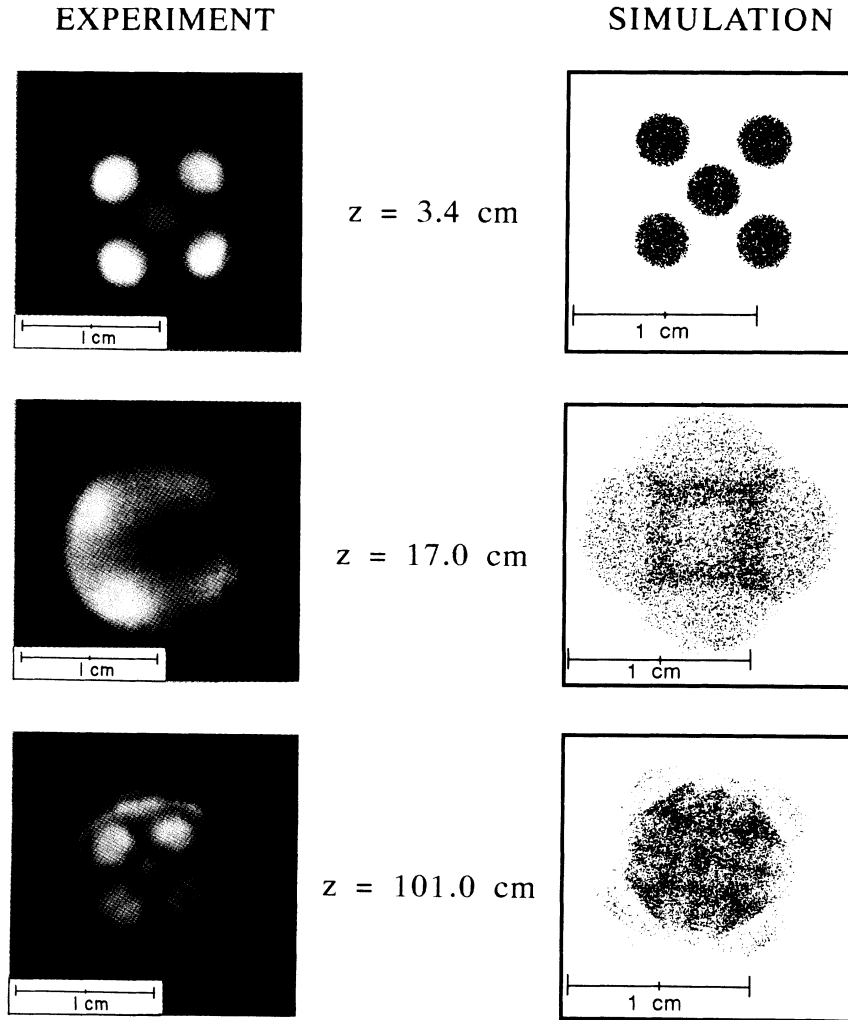


FIG. 2. Phosphor-screen pictures and simulation point plots showing separate beamlets at  $z = 3.4$  cm, merged at  $z = 17$  cm, and image at  $z = 101$  cm.

wavelength  $\lambda$  of the particle oscillations and of the effective emittance of the beam. The trajectory of a particle launched at point  $r_0$  with slope  $r'_0$  can be approximated by

$$r(z) = r_0 \cos(kz) + r'_0 k^{-1} \sin(kz), \quad (8)$$

where  $k = 2\pi/\lambda = \sigma/S$ . The image location  $z_i$  is defined by  $\sin(kz_i) = 0$  or

$$z_i = \frac{m\pi}{k} = \frac{m\pi S}{\sigma} \quad (m = 1, 2, 3, \dots). \quad (9)$$

In our experiment, we observed only the first image ( $m = 1$ ) which occurred at  $z_i/S = 7.5 \pm 1.0$ . This corresponds to a phase advance of  $\sigma = 24.5^\circ \pm 3.0^\circ$ ; hence  $\sigma/\sigma_0 = 0.35 \pm 0.04$ . Given this result for  $\sigma/\sigma_0$ , we can use Eq. (1) and the relation  $R^2 = KS^2/\sigma^2$  to determine the effective emittance of the beam. One finds  $\epsilon_f = 84 \pm 12$  mm-mrad, i.e.,  $\epsilon_f/\epsilon_i = 2.6 \pm 0.4$ , which fits well

with the theoretical and simulation results.

The actual measurement of the emittance at the end of the channel (at  $z = 524$  cm) by the slit-pinhole technique described elsewhere<sup>11</sup> yielded a value of  $\epsilon = 108 \pm 6$  mm-mrad, i.e., a growth factor of  $\epsilon_f/\epsilon_i = 3.3 \pm 0.2$  which is about 20% higher than the simulation results. The higher value can be attributed to matching errors and beam off-centering due to lens misalignments. We conclude, therefore, that the effect has been confirmed experimentally and that there is good agreement between theory, numerical simulation, and experiment.

Finally, we note that charge homogenization and emittance growth occur not only in a focusing channel, but also in drift space. This was, to our knowledge, first pointed out by Blewett<sup>12</sup> in a theoretical study on the expansion of a drifting laminar beam with nonuniform density profile. More recently, Lee, Yu, and Barletta<sup>13</sup> studied this effect in a ballistically focused, drifting

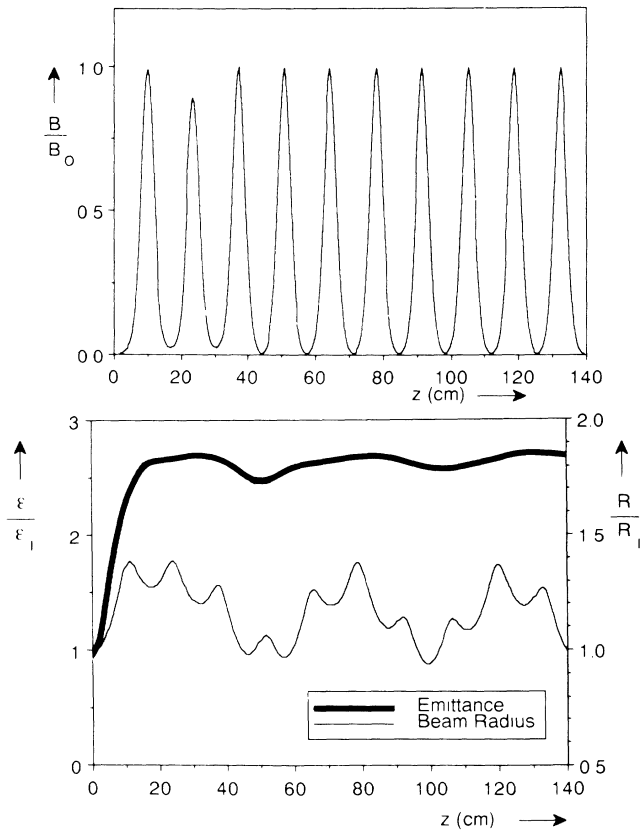


FIG. 3. (Top) Magnetic field variation along beam axis ( $B_0=83.2$  G) used in experiment and simulation runs. (Bottom) Variation of effective beam radius and emittance from simulation.

beam and derived an emittance growth formula analogous to Eq. (3). In our experiment we also observed beamlet merging and charge homogenization when the magnetic field was turned off. However, since the ex-

panding beam hits the drift wall in a distance of about 20 cm, we could not measure the emittance growth in this case.

This research was supported by the Department of Energy and the Office of Naval Research.

(a)Electrical Engineering Department.

(b)Department of Physics and Astronomy.

<sup>1</sup>J. Struckmeier, J. Klabunde, and M. Reiser, *Part. Accel.* **15**, 47 (1984).

<sup>2</sup>T. P. Wangler, K. R. Crandall, R. S. Mills, and M. Reiser, *IEEE Trans. Nucl. Sci.* **32**, 2196 (1985).

<sup>3</sup>O. A. Anderson, *Part. Accel.* **21**, 197 (1987).

<sup>4</sup>I. Hofmann and J. Struckmeier, *Part. Accel.* **21**, 69 (1987).

<sup>5</sup>C. M. Celata, A. Faltens, David L. Judd, L. Smith, and M. G. Tiefenback, in *Proceedings of the 1987 Particle Accelerator Conference, Washington DC, 16-19 March 1987*, edited by E. R. Lindstrom and L. S. Taylor (IEEE, New York, 1987), pp. 1167-1169.

<sup>6</sup>P. M. Lapostolle, *IEEE Trans. Nucl. Sci.* **18**, 1105 (1971).

<sup>7</sup>M. Reiser, *Part. Accel.* **8**, 167 (1978).

<sup>8</sup>J. McAdoo, E. Chojnacki, P. Loschialpo, K. Low, M. Reiser, and J. D. Lawson, *IEEE Trans. Nucl. Sci.* **32**, 2632 (1985).

<sup>9</sup>I. Haber, in *High-Current, High-Brightness, and High-Duty Factor Ion Injectors—1985*, edited by G. H. Gillespie *et al.*, AIP Conference Proceedings No. 139 (American Institute of Physics, New York, 1985), p. 107.

<sup>10</sup>J. D. Lawson, P. M. Lapostolle, and R. L. Gluckstern, *Part. Accel.* **5**, 61 (1973).

<sup>11</sup>M. J. Rhee and R. F. Schneider, *Part. Accel.* **20**, 133 (1986).

<sup>12</sup>J. P. Blewett, "On the Rate of Blow-Up of Dense Particle Beams," Brookhaven National Laboratory Internal Report No. AADD-98, 10 February 1966 (unpublished).

<sup>13</sup>E. P. Lee, S. S. Yu, and W. A. Barletta, *Nucl. Fusion* **21**, 961 (1981).

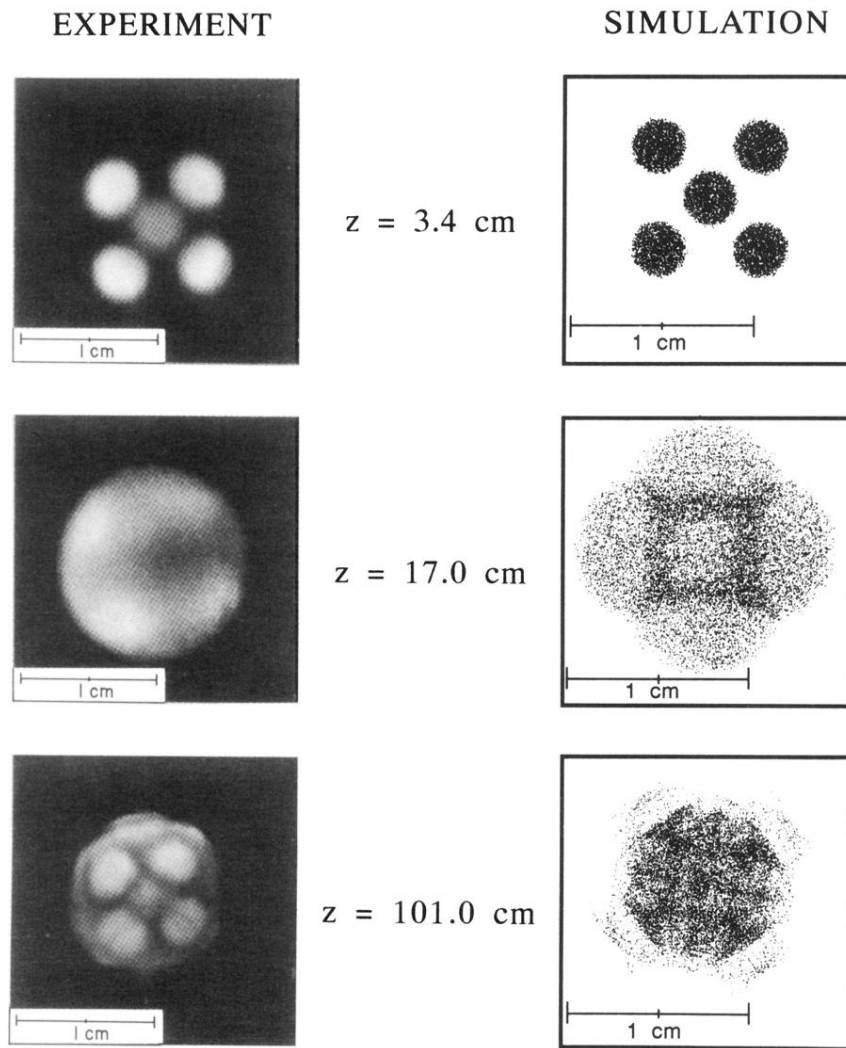


FIG. 2. Phosphor-screen pictures and simulation point plots showing separate beamlets at  $z = 3.4 \text{ cm}$ , merged at  $z = 17 \text{ cm}$ , and image at  $z = 101 \text{ cm}$ .